

# Role of the Delta (1232) in DIS on polarized $^3\text{He}$ and extraction of the neutron spin structure function $g_1^n(x, Q^2)$

C. Boros<sup>a</sup>, V. Guzey<sup>a</sup>, M. Strikman<sup>b</sup>, and A.W. Thomas<sup>a,c</sup>

<sup>a</sup>*Special Research Centre for the Subatomic Structure of Matter (CSSM),*

*Adelaide University, Australia, 5005*

<sup>b</sup>*The Pennsylvania State University, University Park, PA, USA*

<sup>c</sup> *The Department of Physics and Mathematical Physics, Adelaide University, Australia, 5005*

## Abstract

We consider the effect of the transitions  $n \rightarrow \Delta^0$  and  $p \rightarrow \Delta^+$  in deep inelastic scattering on polarized  $^3\text{He}$  on the extraction of the neutron spin structure function  $g_1^n(x, Q^2)$ . Making the natural assumption that these transitions are the dominant non-nucleonic contributions to the renormalization of the axial vector coupling constant in the  $A = 3$  system, we find that the effect of  $\Delta$  increases  $g_1^n(x, Q^2)$  by  $10 \div 40\%$  in the range  $0.05 \leq x \leq 0.6$ , where our considerations are applicable and most of the data for  $g_1^n(x, Q^2)$  exist.

## I. INTRODUCTION

Deep inelastic scattering (DIS) of polarized leptons on polarized targets is used to study the spin structure functions of protons, neutrons, and light nuclei. The spin structure functions carry information about the distribution of the helicity of the target between its constituents. Hence, studies of the spin structure functions are aimed at the understanding

of the spin structure of nucleons and nuclei in terms of the underlying degrees of freedom, quarks and gluons.

This work is concerned with the neutron spin structure function  $g_1^n(x, Q^2)$ . Free neutron targets are not available. Instead, polarized deuterium and  $^3\text{He}$  targets are used as sources of information on the polarized neutron. Considerable experimental information on the structure function  $g_1^n(x, Q^2)$  has been obtained so far. The HERMES collaboration at DESY [1] and the E154 experiment at SLAC [2] used a polarized  $^3\text{He}$  target, while the SMC collaboration at CERN [3] and the E143 experiment at SLAC [4] used polarized deuterium. In both cases the extraction of the neutron structure function  $g_1^n(x, Q^2)$  from the nuclear data required that nuclear effects be taken into account.

The nuclear effects which play a role in polarized and unpolarized DIS on nuclei can be divided into coherent and incoherent contributions. Incoherent nuclear effects result from the scattering of the incoming lepton on each individual nucleon, nucleon resonance, or virtual meson. They are present at all Bjorken  $x$ .

Coherent nuclear effects arise from the interaction of the incoming lepton with two or more nucleons in the target. They are typically concentrated at low values of Bjorken  $x$ . Nuclear shadowing at  $10^{-5} \div 10^{-4} \leq x \leq 0.05$  and antishadowing at  $0.05 \leq x \leq 0.2$  are examples of coherent effects. An analysis of the role of nuclear shadowing and antishadowing as well as the  $\Delta \rightarrow N$  transitions on the extraction of  $g_1^n(x, Q^2)$  from the data on polarized DIS on  $^3\text{He}$  will be presented in a separate publication. In the present work, we do not consider shadowing and antishadowing effects since our main emphasis is on the region of high  $x$ .

For the case of polarized DIS, the major contribution comes from the incoherent scattering on the nucleons of the target. The nucleon-nucleon tensor force gives rise to sizable higher partial waves in bound-state nuclear wave functions, notably the  $D$  wave in the deuteron ground-state wave function as well as the  $S'$  and  $D$  waves in the  $^3\text{He}$  and  $^3\text{H}$  ground-state wave functions. The presence of these partial waves in the nuclear ground-state wave functions leads to spin depolarization (a decrease of the effective polarization)

of the nucleons [5]. In particular, in  $^3\text{He}$  the effective polarization of the neutron is often quoted as  $86 \pm 2\%$ , while the effective polarization of each proton is  $-2.8 \pm 0.4\%$  [6]. These values represent the average of calculations with various nucleon-nucleon potentials and three-nucleon forces. However, the large error bars are very conservative as they have been taken to be 3 times the average value of the spread of the calculated points about the fit to these points [6]. In our analysis, we prefer to use the actual spread of the calculated values, namely,  $P_n = 86 \pm 0.8\%$  and  $P_p = -2.8 \pm 0.15\%$  for the effective polarization of the neutron and the protons, respectively.

The importance of spin depolarization is well established. This effect was taken into account by the experimental collaborations named above when the neutron spin structure function  $g_1^n(x, Q^2)$  was extracted from the DIS data on polarized deuterium and  $^3\text{He}$ . In order to extract the precise shape of  $g_1^n(x, Q^2)$  one must also account for Fermi motion as well as binding and off-shell effects. For deuterium the calculations of Ref. [7] and for  $^3\text{He}$  those of Ref. [8] suggest that simply accounting for spin depolarization is quite a good approximation at  $x \leq 0.7$ .

Until now, other incoherent nuclear effects such as nucleon resonances and meson-exchange currents have been assumed to play a negligible role in polarized DIS. On the other hand, one knows that exchange currents involving the  $\Delta$  resonance play a vital role in explaining the observed axial vector coupling constant of  $^3\text{H}$ . Through the generalization of the Bjorken sum rule to the tri-nucleon system one therefore knows that  $\Delta$  must play a role in the spin structure functions of  $^3\text{He}$  and  $^3\text{H}$ . In this work we analyze the effect of  $\Delta$  on the extraction of  $g_1^n(x, Q^2)$  from  $g_1^{^3\text{He}}(x, Q^2)$ .

## II. THE ROLE OF $\Delta(1232)$ IN POLARIZED DIS ON $^3\text{HE}$

It is well known that exchange currents involving a  $\Delta$  isobar allow one to account for the 4% discrepancy between the experimental value and theoretical predictions for the Gamow-Teller matrix element in triton beta decay [9]. It was observed in Ref. [10] that this 4%

discrepancy straightforwardly translates into the language of deep inelastic scattering on tri-nucleon systems. In particular, calculations with realistic bound-state wave functions of  $^3\text{H}$  and  $^3\text{He}$  involving nucleons alone, underestimate the ratio of the Bjorken sum rules for the tri-nucleon system and for the nucleon by the same amount.

The Bjorken sum rule was derived using the algebra of currents [11]. It reads

$$\int_0^1 \left( g_1^p(x, Q^2) - g_1^n(x, Q^2) \right) dx = \frac{1}{6} g_A \left( 1 + O\left(\frac{\alpha_s}{\pi}\right) \right), \quad (1)$$

where  $g_A$  is the axial vector coupling constant measured in the  $\beta$  decay of neutron,  $g_A = 1.2670 \pm 0.0035$  [12]. The QCD radiative corrections to this sum rule were calculated in perturbative QCD using the Operator Product Expansion. They are denoted by “ $O(\alpha_s/\pi)$ ”.

Analogously, one can write for the difference of the spin structure functions of  $^3\text{H}$  and  $^3\text{He}$

$$\int_0^1 \left( g_1^{^3H}(x, Q^2) - g_1^{^3He}(x, Q^2) \right) dx = \frac{1}{6} g_A|_{triton} \left( 1 + O\left(\frac{\alpha_s}{\pi}\right) \right), \quad (2)$$

where  $g_A|_{triton}$  is the axial vector coupling constant measured in the  $\beta$  decay of triton,  $g_A|_{triton} = 1.211 \pm 0.002$  [13].

Taking the ratio of Eqs. (1) and (2), one obtains

$$\eta \equiv \frac{g_A|_{triton}}{g_A} = \frac{\int_0^1 \left( g_1^{^3H}(x, Q^2) - g_1^{^3He}(x, Q^2) \right) dx}{\int_0^1 \left( g_1^p(x, Q^2) - g_1^n(x, Q^2) \right) dx} = 0.956 \pm 0.004. \quad (3)$$

Note that in Eq. (3) the QCD radiative corrections cancel exactly.

On the other hand, calculations with exact wave functions of the tri-nucleon system involving only nucleons predict that

$$\begin{aligned} & \int \left( g_1^{^3H}(x, Q^2) - g_1^{^3He}(x, Q^2) \right) dx = \\ & \left( 1 - \frac{4}{3} P_{S'} - \frac{2}{3} P_D \right) \int \left( g_1^p(x, Q^2) - g_1^n(x, Q^2) \right) dx \equiv \\ & (P_n - 2P_p) \int \left( g_1^p(x, Q^2) - g_1^n(x, Q^2) \right) dx, \end{aligned} \quad (4)$$

where  $P_{S'}$  and  $P_D$  are the probabilities of the corresponding partial waves in the bound-state wave function of  $^3\text{He}$ . Using  $P_n = 0.86 \pm 0.008$  and  $2P_p = -0.056 \pm 0.003$  and substituting Eq. (4) into Eq. (3) one obtains

$$\frac{\int_0^1 (g_1^{3H}(x, Q^2) - g_1^{3He}(x, Q^2)) dx}{\int_0^1 (g_1^p(x, Q^2) - g_1^n(x, Q^2)) dx} = 0.916 \pm 0.009 . \quad (5)$$

In Eq. (5) the errors for  $P_n$  and  $2P_p$  are not correlated and therefore have been added in quadrature.

By comparing Eqs. (3) and (5) one can see that calculations of the structure functions  $g_1^{3H}(x, Q^2)$  and  $g_1^{3He}(x, Q^2)$  based on nucleons alone underestimate the quenching factor  $\eta$  in Eq. (3) by about 4%.

As explained above, it is natural to expect that this discrepancy can be accounted for by including the DIS diagrams which correspond to the transitions  $n \rightarrow \Delta^0$  and  $p \rightarrow \Delta^+$ . This corresponds precisely to the two-body exchange currents involving the  $\Delta$  which appear in calculations of the Gamow-Teller matrix element for the triton beta decay. Fig. 1 demonstrates the correspondence between the interference diagrams in polarized DIS and the two-body exchange currents involving a  $\Delta$  entering the Gamow-Teller matrix element calculations.

In Ref. [9] was shown that the contribution of the diagrams of Fig. 1 increases the theoretical prediction of the axial vector coupling constant of the triton by 4% and makes it consistent with the experimental value. By analogy, we assume that the contribution of the interference terms,  $n \rightarrow \Delta^0$  and  $p \rightarrow \Delta^+$ , in polarized DIS will make the theoretical prediction of Eq. (5) equal to the experimental value of Eq. (3).

Note also that the contribution of the DIS diagrams involving the transition  $\Delta \rightarrow \Delta$  is neglected since the contribution of the corresponding diagrams to triton beta decay is negligible.

Taking into account the interference terms in polarized DIS on tri-nucleon systems, the spin structure functions of  $^3\text{He}$  and  $^3\text{H}$  can be expressed as

$$\begin{aligned} g_1^{3He}(x, Q^2) &= \int_x^A \frac{dy}{y} \Delta f_{n/3He}(y) g_1^n(x/y, Q^2) + \int_x^A \frac{dy}{y} \Delta f_{p/3He}(y) g_1^p(x/y, Q^2) + \\ &+ \int_x^A \frac{dy}{y} \Delta f_{n \rightarrow \Delta^0/3He}(y) g_1^{n \rightarrow \Delta^0}(x/y, Q^2) + \int_x^A \frac{dy}{y} \Delta f_{p \rightarrow \Delta^+/3He}(y) g_1^{p \rightarrow \Delta^+}(x/y, Q^2) , \\ g_1^{3H}(x, Q^2) &= \int_x^A \frac{dy}{y} \Delta f_{n/3H}(y) g_1^n(x/y, Q^2) + \int_x^A \frac{dy}{y} \Delta f_{p/3H}(y) g_1^p(x/y, Q^2) + \end{aligned}$$

$$+ \int_x^A \frac{dy}{y} \Delta f_{n \rightarrow \Delta^0 / ^3H}(y) g_1^{n \rightarrow \Delta^0}(x/y, Q^2) + \int_x^A \frac{dy}{y} \Delta f_{p \rightarrow \Delta^+ / ^3H}(y) g_1^{p \rightarrow \Delta^+}(x/y, Q^2) , \quad (6)$$

where  $\Delta f_{n/^3He}(y)$  ( $\Delta f_{n/^3H}(y)$ ),  $\Delta f_{p/^3He}(y)$  ( $\Delta f_{p/^3H}(y)$ ),  $\Delta f_{n \rightarrow \Delta^0 / ^3He}(y)$  ( $\Delta f_{n \rightarrow \Delta^0 / ^3H}(y)$ ), and  $\Delta f_{p \rightarrow \Delta^+ / ^3He}(y)$  ( $\Delta f_{p \rightarrow \Delta^+ / ^3H}(y)$ ) are the spin-dependent light-cone momentum distributions of the neutron, proton,  $n \rightarrow \Delta^0$ , and  $p \rightarrow \Delta^+$  interference terms in  $^3\text{He}$  ( $^3\text{H}$ ), respectively;  $g_1^{n \rightarrow \Delta^0}(x, Q^2)$  and  $g_1^{p \rightarrow \Delta^+}(x, Q^2)$  are the spin structure functions of the corresponding interference terms.

In the approximation where Fermi motion and off-shell effects are negligible so  $\Delta f_{i/^3He}(y) \propto \delta(y - 1)$  ( $\Delta f_{i/^3H}(y) \propto \delta(y - 1)$ ) we find

$$\begin{aligned} g_1^{^3He}(x, Q^2) &= P_n g_1^n(x, Q^2) + 2P_p g_1^p(x, Q^2) \\ &+ 2P_{n \rightarrow \Delta^0} g_1^{n \rightarrow \Delta^0}(x, Q^2) + 4P_{p \rightarrow \Delta^+} g_1^{p \rightarrow \Delta^+}(x, Q^2) , \\ g_1^{^3H}(x, Q^2) &= P_n g_1^n(x, Q^2) + 2P_p g_1^p(x, Q^2) \\ &- 2P_{n \rightarrow \Delta^0} g_1^{n \rightarrow \Delta^0}(x, Q^2) - 4P_{p \rightarrow \Delta^+} g_1^{p \rightarrow \Delta^+}(x, Q^2) . \end{aligned} \quad (7)$$

In Eq. (7)  $P_{n \rightarrow \Delta^0}$  and  $P_{p \rightarrow \Delta^+}$  stand for the effective polarization of the interference transitions  $n \rightarrow \Delta^0$  and  $p \rightarrow \Delta^+$  in  $^3\text{He}$ , respectively. Additional factors of two in front of the interference terms correspond to the sum of the  $N \rightarrow \Delta$  and  $\Delta \rightarrow N$  transitions. The minus sign in front of the interference term contribution to  $g_1^{^3H}(x, Q^2)$  originates due to the sign convention

$$\begin{aligned} P_{n \rightarrow \Delta^0} &\equiv P_{n \rightarrow \Delta^0 / ^3He} = -P_{p \rightarrow \Delta^+ / ^3H} , \\ P_{p \rightarrow \Delta^+} &\equiv P_{p \rightarrow \Delta^+ / ^3He} = -P_{n \rightarrow \Delta^0 / ^3H} . \end{aligned} \quad (8)$$

In the next section we shall make predictions for spin structure functions  $g_1^{n \rightarrow \Delta^0}(x, Q^2)$  and  $g_1^{p \rightarrow \Delta^+}(x, Q^2)$  using the quark model and estimate the effective polarizations  $P_{n \rightarrow \Delta^0}$  and  $P_{p \rightarrow \Delta^+}$  using Eq. (3) as a guide.

### III. INTERFERENCE SPIN STRUCTURE FUNCTIONS AND THE EFFECTIVE POLARIZATIONS

The contribution to the nuclear spin structure functions associated with the  $\Delta \rightarrow N$  and  $N \rightarrow \Delta$  interference terms,  $g_1^{n \rightarrow \Delta^0}(x, Q^2)$  and  $g_1^{p \rightarrow \Delta^+}(x, Q^2)$ , can be calculated within the framework of the valence quark model. Since only valence quarks are present in this picture, the model, and hence, our predictions for the interference spin structure functions  $g_1^{n \rightarrow \Delta^0}(x, Q^2)$  and  $g_1^{p \rightarrow \Delta^+}(x, Q^2)$  are valid where the valence parton picture is applicable. The following simple analysis shows that polarized valence quarks dominate over polarized sea quarks at  $Q^2 \leq 4 \text{ GeV}^2$  and not very low  $x$ . Using the parameterization of spin-dependent parton distributions from Ref. [14], one can readily check that polarized distribution for valence  $u$  and  $d$  quarks are larger than the polarized sea quark distributions in the range  $0.34 \leq Q^2 \leq 4 \text{ GeV}^2$  and  $0.05 \leq x \leq 0.8$  by at least a factor of five. This justifies the use of the valence (constituent) quark picture at these values of  $Q^2$  and  $x$ .

The probabilities to find polarized *up*, *down*, and *strange* quarks for the octet of baryons, the decuplet of baryon resonances and the interference between octet and decuplet states were derived in Ref. [15], using SU(6) wave functions with energies perturbed by the standard spin-dependent hyperfine interactions [16] – following earlier work for the nucleon [17].

The spin structure function  $g_1(x, Q^2)$  for the proton and neutron, and the interference terms,  $p \rightarrow \Delta^+$  and  $n \rightarrow \Delta^0$ , within the framework of the valence quark parton model is defined as

$$g_1(x, Q^2) = \frac{1}{2} \left( \frac{4}{9} \Delta u(x, Q^2) + \frac{1}{9} \Delta d(x, Q^2) \right), \quad (9)$$

where  $\Delta u(x, Q^2) \equiv u^\uparrow(x, Q^2) - u^\downarrow(x, Q^2)$  and  $\Delta d(x, Q^2) \equiv d^\uparrow(x, Q^2) - d^\downarrow(x, Q^2)$ ;  $u^\uparrow(x, Q^2)$  ( $d^\uparrow(x, Q^2)$ ) and  $u^\downarrow(x, Q^2)$  ( $d^\downarrow(x, Q^2)$ ) are the probabilities to find the up (down) quark with helicity parallel and antiparallel, respectively, to the helicity of the target.

Using the results of Ref. [15] and the definition (9) one can express the spin structure functions for the proton and neutron as well as the interference terms,  $p \rightarrow \Delta^+$  and  $n \rightarrow \Delta^0$ , at some initial scale  $Q_0$  as

$$\begin{aligned}
g_1^p(x, Q_0^2) &= \frac{1}{18} \left( 6G_s(x, Q_0^2) - G_v(x, Q_0^2) \right) , \\
g_1^n(x, Q_0^2) &= \frac{1}{12} \left( G_s(x, Q_0^2) - G_v(x, Q_0^2) \right) , \\
g_1^{p \rightarrow \Delta^+}(x, Q_0^2) &= \frac{\sqrt{2}}{9} G_v(x, Q_0^2) , \\
g_1^{n \rightarrow \Delta^0}(x, Q_0^2) &= \frac{\sqrt{2}}{9} G_v(x, Q_0^2) , 
\end{aligned} \tag{10}$$

where  $G_s(x, Q_0^2)$  and  $G_v(x, Q_0^2)$  are the contributions to the spin structure functions associated with a pair of spectator quarks in the baryon wave function with  $S = 0, I = 0$  and  $S = 1, I = 1$ , respectively. These contributions can be calculated using, for example, the MIT Bag model with  $Q_0^2 = 0.23 \text{ GeV}^2$ , as was done in Ref. [15].

One can also derive a sum rule, analogous to the Bjorken sum rule, which relates in a model-independent way the sum of the first moments of  $g_1^{p \rightarrow \Delta^+}(x, Q^2)$  and  $g_1^{n \rightarrow \Delta^0}(x, Q^2)$  to a certain axial current matrix element. The derivation is completely analogous to the one for the Bjorken sum rule. That is, the operator product expansion or algebra of currents relates the commutator of two electromagnetic currents, whose matrix element defines the usual hadronic electromagnetic tensor  $W_{\mu\nu}$  of DIS, to the axial current. Sandwiching this commutator between baryon states and using an unsubtracted dispersion relation for the structure function  $g_1(x, Q^2)$  constrains the integral  $\int g_1(x, Q^2) dx$ . If we choose the initial state to be a nucleon and the final state to be a  $\Delta(1232)$  resonance we arrive at the following relationships

$$\begin{aligned}
\int_0^1 g_1^{p \rightarrow \Delta^+}(x, Q^2) dx &= \frac{1}{2} B_1^{p \rightarrow \Delta^+} \left( 1 + O\left(\frac{\alpha_s}{\pi}\right) \right) , \\
\int_0^1 g_1^{n \rightarrow \Delta^0}(x, Q^2) dx &= \frac{1}{2} B_1^{n \rightarrow \Delta^0} \left( 1 + O\left(\frac{\alpha_s}{\pi}\right) \right) . 
\end{aligned} \tag{11}$$

The matrix elements  $B_1$  are defined as

$$\begin{aligned}
2 s^\mu B_1^{p \rightarrow \Delta^+} &\equiv \langle \Delta^+, s | \frac{4}{9} \bar{u} \gamma^\mu \gamma_5 u + \frac{1}{9} \bar{d} \gamma^\mu \gamma_5 d | p, s \rangle , \\
2 s^\mu B_1^{n \rightarrow \Delta^0} &\equiv \langle \Delta^0, s | \frac{4}{9} \bar{u} \gamma^\mu \gamma_5 u + \frac{1}{9} \bar{d} \gamma^\mu \gamma_5 d | n, s \rangle , 
\end{aligned} \tag{12}$$

where  $s^\mu$  is the polarization vector of the nucleon and  $\Delta$  defined as in Ref. [18].



Using the representation of the wave functions of the proton, neutron, and  $\Delta$  in terms of quark fields and the standard commutation relationships between the quark fields one can relate the sum of the matrix elements  $B_1^{p \rightarrow \Delta^+}$  and  $B_1^{n \rightarrow \Delta^0}$  to the axial vector coupling constant for the beta decay  $\nu_\mu p \rightarrow \mu^- \Delta^{++}$ . Decomposing the electromagnetic current in Eq. (12) into isovector and isoscalar components one can readily obtain

$$\begin{aligned}\langle \Delta^+, s | \bar{u} \gamma^\mu \gamma_5 u - \bar{d} \gamma^\mu \gamma_5 d | p, s \rangle &= -2 \langle \Delta^+, s | \bar{u} \gamma^\mu \gamma_5 d | n, s \rangle, \\ \langle \Delta^0, s | \bar{u} \gamma^\mu \gamma_5 u - \bar{d} \gamma^\mu \gamma_5 d | n, s \rangle &= -2 \langle \Delta^+, s | \bar{u} \gamma^\mu \gamma_5 d | n, s \rangle.\end{aligned}\quad (13)$$

It also follows from Ref. [15] that

$$\begin{aligned}\langle \Delta^+, s | \bar{u} \gamma^\mu \gamma_5 u + \bar{d} \gamma^\mu \gamma_5 d | p, s \rangle &= 0, \\ \langle \Delta^0, s | \bar{u} \gamma^\mu \gamma_5 u + \bar{d} \gamma^\mu \gamma_5 d | n, s \rangle &= 0.\end{aligned}\quad (14)$$

Using Eqs. (12), (13), and (14) one can write

$$2 s^\mu (B_1^{p \rightarrow \Delta^+} + B_1^{n \rightarrow \Delta^0}) = -\frac{2}{3} \langle \Delta^+, s | \bar{u} \gamma^\mu \gamma_5 d | n, s \rangle. \quad (15)$$

The commutation relationships between the quark fields relate the latter matrix element to the effective axial vector coupling constant in the reaction  $\nu_\mu p \rightarrow \mu^- \Delta^{++}$ ,  $g_A(p \rightarrow \Delta^{++})$ :

$$\langle \Delta^+, s | \bar{u} \gamma^\mu \gamma_5 d | n, s \rangle = -\frac{1}{\sqrt{3}} \langle \Delta^{++}, s | \bar{u} \gamma^\mu \gamma_5 d | p, s \rangle \equiv -\frac{1}{\sqrt{3}} 2 s^\mu g_A(p \rightarrow \Delta^{++}). \quad (16)$$

Combining Eqs. (15), (16), and (11) one obtains the following sum rule

$$\int_0^1 \left( g_1^{p \rightarrow \Delta^+}(x, Q^2) + g_1^{n \rightarrow \Delta^0}(x, Q^2) \right) dx = \frac{1}{3\sqrt{3}} g_A(p \rightarrow \Delta^{++}) \left( 1 + O\left(\frac{\alpha_s}{\pi}\right) \right). \quad (17)$$

The sum rule (17) is exact (modulo the QCD radiative corrections) in the limit of SU(6) symmetry. Indeed, in this case  $\int_0^1 G_v(x, Q_0^2) dx = 1$  and the left hand side of Eq. (17) equals  $2\sqrt{2}/9$ . On the other hand,  $g_A(p \rightarrow \Delta^{++}) = 2\sqrt{2/3}$  [19] and the right hand side of Eq. (17) equals  $2\sqrt{2}/9$  too.

We also expect that SU(6) should be a good approximation for the right hand side of Eq. (17) because it works qualitatively well for the form factor  $C_5^A(0)$  associated with the

reaction  $\nu_\mu p \rightarrow \mu^- \Delta^{++}$ . The theoretical analysis of Ref. [20] of the experimental data from the BNL experiment [21] found that  $C_5^A(0) = 1.22 \pm 0.06$ . This value is close to the SU(6) prediction,  $C_5^A(0) = 1.15$ .

In order to successfully apply Eq. (7) to extract the neutron spin structure function  $g_1^n(x, Q^2)$  from the  $^3\text{He}$  data one needs to address two issues: the effective polarizations of the interference terms,  $P_{n \rightarrow \Delta^0}$  and  $P_{p \rightarrow \Delta^+}$  and the  $Q^2$  and  $x$  dependence of the spin structure functions of the interference terms,  $g_1^{n \rightarrow \Delta^0}(x, Q^2)$  and  $g_1^{p \rightarrow \Delta^+}(x, Q^2)$ .

The first question can be readily answered using the sum rule (17). Substituting Eqs. (7) into Eq. (3) and using Eq. (5) one obtains

$$0.956 = 0.916 + 2(P_{n \rightarrow \Delta^0} + 2P_{p \rightarrow \Delta^+}) \frac{\int_0^1 dx (g_1^{n \rightarrow \Delta^0}(x, Q^2) + g_1^{p \rightarrow \Delta^+}(x, Q^2))}{\int_0^1 dx (g_1^n(x, Q^2) - g_1^p(x, Q^2))}. \quad (18)$$

We have assumed that the QCD radiative corrections in Eq. (18) cancel.

Since we have assumed that the contributions of the  $n \rightarrow \Delta^0$  and  $p \rightarrow \Delta^+$  transitions make the theoretical prediction and the experimental value of  $g_A|_{\text{triton}}$  consistent, the effective polarizations of the interference terms,  $P_{n \rightarrow \Delta^0}$  and  $P_{p \rightarrow \Delta^+}$ , should be such that Eq. (18) is satisfied. Thus, using the sum rule (17) and Eq. (18) one can write

$$2(P_{n \rightarrow \Delta^0} + 2P_{p \rightarrow \Delta^+}) = -\sqrt{3} \times 0.04 \frac{g_A}{g_A(p \rightarrow \Delta^{++})} = -0.027. \quad (19)$$

In Eq. (19) we have assumed the SU(6) value for  $g_A(p \rightarrow \Delta^{++})$ , namely  $g_A(p \rightarrow \Delta^{++}) = 2\sqrt{2/3}$ .

Therefore, the spin structure function  $g_1^{^3\text{He}}(x, Q^2)$  of Eq. (7) can be written as

$$g_1^{^3\text{He}}(x, Q^2) = P_n g_1^n(x, Q^2) + 2P_p g_1^p(x, Q^2) - 0.027 g_1^{n \rightarrow \Delta^0}(x, Q^2). \quad (20)$$

We stress that Eq. (20) is an approximation which neglects Fermi motion and off-shell effects.

Next we need to know the interference structure function,  $g_1^{n \rightarrow \Delta^0}(x, Q^2)$ , as a function of  $Q^2$  and  $x$ . In Ref. [15]  $G_s(x, Q^2)$  and  $G_v(x, Q^2)$  which enter Eq. (10) were evaluated within the framework of the MIT Bag model. Then, in order to make a comparison to other parameterizations of polarized quark densities and to spin structure functions, the QCD evolution from the bag scale  $Q_0^2 = 0.23 \text{ GeV}^2$  to large  $Q^2$  was performed.

Instead of using a particular model for  $G_s(x, Q^2)$  and  $G_v(x, Q^2)$  and then performing the QCD evolution, one can relate  $g_1^{n \rightarrow \Delta^0}(x, Q^2)$  to  $g_1^p(x, Q^2)$  and  $g_1^n(x, Q^2)$  in a model-independent way. Using Eq. (10) one can write

$$g_1^{p \rightarrow \Delta^+}(x, Q^2) = g_1^{n \rightarrow \Delta^0}(x, Q^2) = \frac{2\sqrt{2}}{5} (g_1^p(x, Q^2) - 4g_1^n(x, Q^2)) . \quad (21)$$

Since Eq. (21) is based solely on the Clebsh-Gordon coefficients used to construct the nucleon and  $\Delta$  wave functions, it holds regardless of whether the SU(6) symmetry of the baryon wave functions is broken or not. Eq. (21) should be valid at all  $x$  and  $Q^2$  where the picture of nucleons and  $\Delta$ 's being composed of valence quarks holds. No information about the dynamics of valence quarks, or information on  $G_s(x, Q^2)$  and  $G_v(x, Q^2)$ , is needed.

Using Eq. (21) in Eq. (20) one can write the following master equation for the spin structure function  $g_1^{3He}(x, Q^2)$

$$g_1^{3He}(x, Q^2) = P_n g_1^n(x, Q^2) + 2P_p g_1^p(x, Q^2) - 0.027 \frac{2\sqrt{2}}{5} (g_1^p(x, Q^2) - 4g_1^n(x, Q^2)) . \quad (22)$$

Eq. (22) describes  $g_1^{3He}(x, Q^2)$  as a sum of the contributions from the effective polarizations of the neutron and proton and the contribution of the interference terms  $N \rightarrow \Delta$  and  $\Delta \rightarrow N$ . As explained above, Eq. (22) neglects Fermi motion and off-shell effects, which is expected to be a good approximation for  $x \leq 0.7$ .

#### IV. EXTRACTION OF $g_1^n(x, Q^2)$ FROM $^3\text{He}$ DATA

Eq. (22) can be used estimate the role played by a  $\Delta$  in extracting the neutron spin structure function  $g_1^n(x, Q^2)$  from the DIS data taken on a polarized  $^3\text{He}$  target.

Let us denote  $g_{1exp}^n(x, Q^2)$  the neutron spin structure function obtained from Eq. (22) when the contribution of the  $\Delta$  is omitted

$$g_1^{3He}(x, Q^2) = P_n g_{1exp}^n(x, Q^2) + 2P_p g_1^p(x, Q^2) . \quad (23)$$

Combining Eqs. (22) and (23) we find the relationship between the theoretical prediction for  $g_1^n(x, Q^2)$  when the effect of the  $\Delta$  is present and  $g_{1exp}^n(x, Q^2)$

$$g_1^n(x, Q^2) = \left( g_{1exp}^n(x, Q^2) + \frac{0.027}{P_n} \frac{2\sqrt{2}}{5} g_1^p(x, Q^2) \right) \times \left( 1 + \frac{0.027}{P_n} \frac{8\sqrt{2}}{5} \right)^{-1} = 0.934 \left( g_{1exp}^n(x, Q^2) + 0.0178 g_1^p(x, Q^2) \right). \quad (24)$$

One can also represent the result of Eq. (24) in the form of the ratio  $g_1^n(x, Q^2)/g_{1exp}^n(x, Q^2)$

$$\frac{g_1^n(x, Q^2)}{g_{1exp}^n(x, Q^2)} = 0.934 + 0.0178 \frac{g_1^p(x, Q^2)}{g_{1exp}^n(x, Q^2)}. \quad (25)$$

In order to demonstrate the magnitude of the nuclear effect associated with the  $\Delta$  we show in Fig. 2 the ratio  $g_1^n(x, Q^2)/g_{1exp}^n(x, Q^2)$  of Eq. (25) as a function of  $x$ . The solid line corresponds to the parameterization of spin-dependent parton densities of Ref. [14] at the initial scale  $Q_0^2=0.23 \text{ GeV}^2$ . The dotted line corresponds to the parameterization of Ref. [22] at a higher initial scale  $Q_0^2=4 \text{ GeV}^2$ . The considered ratio would be unity if the effect of the  $\Delta$  were unimportant. However, from Fig. 2 one can see that the contributions of the interference terms,  $N \rightarrow \Delta$  and  $\Delta \rightarrow N$ , do modify the neutron spin structure function  $g_{1exp}^n(x, Q^2)$  – it is reduced by approximately 7% in the range  $0.05 \leq x \leq 0.1 \div 0.2$  and drops significantly for  $x > 0.1 \div 0.2$  when the parameterization of Ref. [14] is used. The tendency is similar for the parameterization of Ref. [22].

Using Eq. (24) one can also estimate the change in the first moment of  $g_1^n(x, Q^2)$ . Assuming that the effects associated with the  $\Delta$  are present at  $0.05 \leq x \leq 0.8$  in Eq. (24) one finds

$$\begin{aligned} \int_0^1 g_{1exp}^n(x, Q_0^2) dx &= -0.0621, \\ \int_0^1 g_1^n(x, Q_0^2) dx &= -0.0574 \end{aligned} \quad (26)$$

for the parameterization of Ref. [14] at  $Q_0^2=0.23 \text{ GeV}^2$ , and

$$\begin{aligned} \int_0^1 g_{1exp}^n(x, Q_0^2) dx &= -0.0574, \\ \int_0^1 g_1^n(x, Q_0^2) dx &= -0.0540 \end{aligned} \quad (27)$$

for the parameterization of Ref. [22] at  $Q_0^2=4 \text{ GeV}^2$ . For the two parameterizations of spin-dependent parton densities considered here, the contribution of the interference  $N \rightarrow \Delta$  and  $\Delta \rightarrow N$  terms changes the first moment of  $g_1^n(x, Q^2)$  by 8% and 6%, respectively.

Eqs. (24) and (25) can be used in order to re-analyze the extraction of the neutron spin structure function  $g_1^n(x, Q^2)$  from the  $^3\text{He}$  DIS data. The results are presented in Figs. 3, 4, 5 and 6.

Figure 3 represents the values of  $g_{1exp}^n(x, Q^2)$  reported by the E154 collaboration [2] as solid dots, with corresponding error bars, and the theoretical prediction for  $g_1^n(x, Q^2)$  of Eq. (3) as open circles. (The open circles have been shifted to the right in order to make them legible on the plot.) The error bars are purely statistical uncertainties and  $Q^2=5 \text{ GeV}^2$  for each point. The values of  $g_1^p(x, Q^2)$  needed for Eq. (24), at appropriate values of  $x$  and  $Q^2=5 \text{ GeV}^2$ , were taken from the data of the SLAC E143 experiment [4]. From Fig. 3 one can see that the effect of the  $\Delta$  on the extraction of  $g_1^n(x, Q^2)$  from the  $^3\text{He}$  data is to increase the values of  $g_1^n(x, Q^2)$  by  $12 \div 20\%$  in the range  $0.05 \leq x \leq 0.34$ , which is still within the experimental error bars. At  $x > 0.34$  the correction due to the  $\Delta$  is of order  $20 \div 40\%$ . However, the error bars for the corresponding values of  $g_{1exp}^n(x, Q^2)$  are so large that it does not seem sensible to discuss any comparison with the data for  $x > 0.34$ , at present. Note, however, that high precision measurements with the polarized  $^3\text{He}$  target are planned at TJNAF for the  $0.33 \leq x \leq 0.63$  region [23].

The information in Fig. 3 is presented in terms of the ratio of Eq. (25) in Fig. 4. The error bars are systematic uncertainties of experimental values for  $g_1^n(x, Q^2)$  and  $g_1^p(x, Q^2)$  added in quadrature.

In Figs. 5 and 6 we analogously re-analyze the HERMES data Ref. [1]. Note that the data points in Ref. [1] have not been evolved to a common  $Q^2$ . Thus, in Figs. 5 and 6 the values of  $Q^2$  and  $x$  are correlated. We used the HERMES proton data [24] for  $g_1^p(x, Q^2)$  in order to use in Eq. (24) since the values of  $\langle x \rangle$  and  $\langle Q^2 \rangle$  presented are very close to those of Ref. [1]. In order to have  $g_1^p(x, Q^2)$  at exactly the same bins in  $\langle Q^2 \rangle$  as for  $g_1^n(x, Q^2)$  we have extrapolated  $g_1^p(x, Q^2)$  to the required  $\langle Q^2 \rangle$  using the experimentally justified assumption that the ratio  $g_1^p(x, Q^2)/F_1^p(x, Q^2)$  is  $Q^2$ -independent [25]. The spin-independent structure function  $F_1^p(x, Q^2)$  was parameterized using the recent world averaged fits for  $R(x, Q^2)$  [26] and  $F_2^p(x, Q^2)$  [27]. One can see from Figs. 5 and 6 that the contribution of the interference

terms increases  $g_1^n(x, Q^2)$  by  $10 \div 25\%$ , which is so far within the experimental error bars.

## V. CONCLUSIONS

In this work we considered a novel nuclear contribution which affects the extraction of the neutron spin structure function  $g_1^n(x, Q^2)$  from the polarized DIS data on  ${}^3\text{He}$ . The Feynman diagrams which describe deep inelastic scattering on polarized  ${}^3\text{He}$  are analogous to the diagrams which enter the calculation of the Gamow-Teller matrix element of the tritium beta decay. Thus, it is very natural to assume that the diagrams associated with the transitions  $n \rightarrow \Delta^0$  and  $p \rightarrow \Delta^+$  play an important role in polarized DIS on  ${}^3\text{He}$ , because two-body exchange currents involving  $\Delta$  isobars are important in calculations of the Gamow-Teller matrix element.

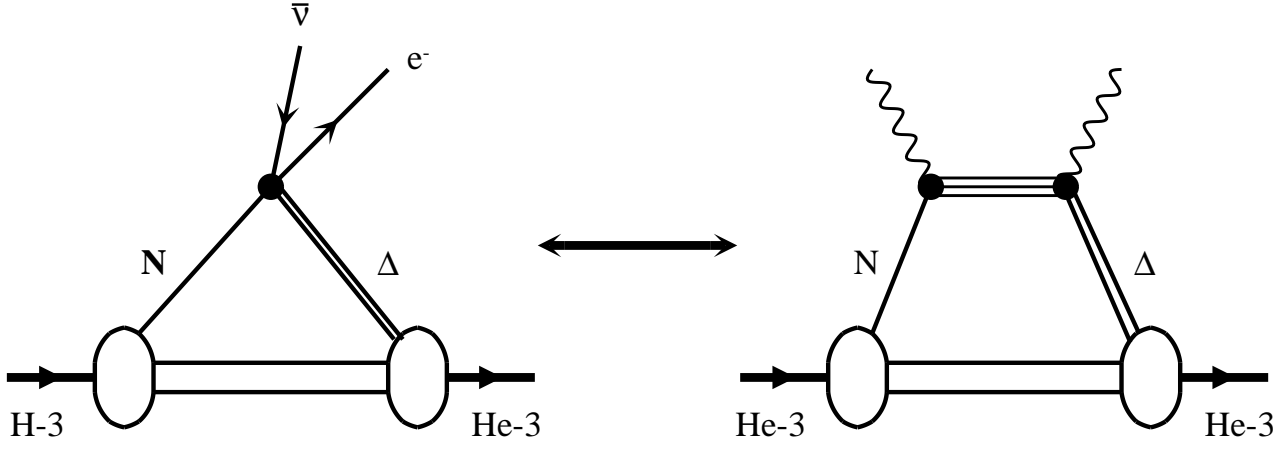
The contributions of the interference transitions  $n \rightarrow \Delta^0$  and  $p \rightarrow \Delta^+$  to the spin structure function of  ${}^3\text{He}$ ,  $g_1^{3\text{He}}(x, Q^2)$ , are characterized by the interference spin structure functions  $g_1^{n \rightarrow \Delta^0}(x, Q^2)$  and  $g_1^{p \rightarrow \Delta^+}(x, Q^2)$ , and effective polarizations  $P_{n \rightarrow \Delta^0}$  and  $P_{p \rightarrow \Delta^+}$ , respectively. A new sum rule for  $g_1^{n \rightarrow \Delta^0}(x, Q^2)$  and  $g_1^{p \rightarrow \Delta^+}(x, Q^2)$  has been derived. We also related  $g_1^{n \rightarrow \Delta^0}(x, Q^2)$  and  $g_1^{p \rightarrow \Delta^+}(x, Q^2)$  to  $g_1^n(x, Q^2)$  and  $g_1^p(x, Q^2)$  within the framework of the valence quark model. The connection to the calculations of the triton beta decay enabled an estimate of the effective polarizations of the interference terms,  $P_{n \rightarrow \Delta^0}$  and  $P_{p \rightarrow \Delta^+}$ , by requiring that the generalization of the Bjorken sum rule to the tri-nucleon system be consistent with the measured axial coupling constant in the  $A = 3$  system.

Taking the effect of the  $\Delta$  into account, we have re-analyzed the neutron spin structure function  $g_1^n(x, Q^2)$  using the data of the E143 and HERMES experiments. We found that, depending on  $x$ , the values of  $g_1^n(x, Q^2)$  increase by  $10 \div 40\%$ . We also estimated that the first moment of  $g_1^n(x, Q^2)$  increases by  $6 \div 8\%$ .

## **VI. ACKNOWLEDGEMENTS**

V.G. would like to thank Kazuo Tsushima for many useful discussions and pointing to Refs. [20] and [21]. This work was partially supported by the Australian Research Counsel and the Department of Energy of the United States of America.

# FIGURES



Triton beta decay

Polarized DIS on He-3

FIG. 1. This figure demonstrates the correspondence between the Feynman diagrams describing the two-body exchange currents involving the  $\Delta$  isobar which appear in calculations of the triton beta decay and the diagrams involving the  $n \rightarrow \Delta^0$  and  $p \rightarrow \Delta^+$  transitions which contribute to the polarized DIS on  ${}^3\text{He}$ .



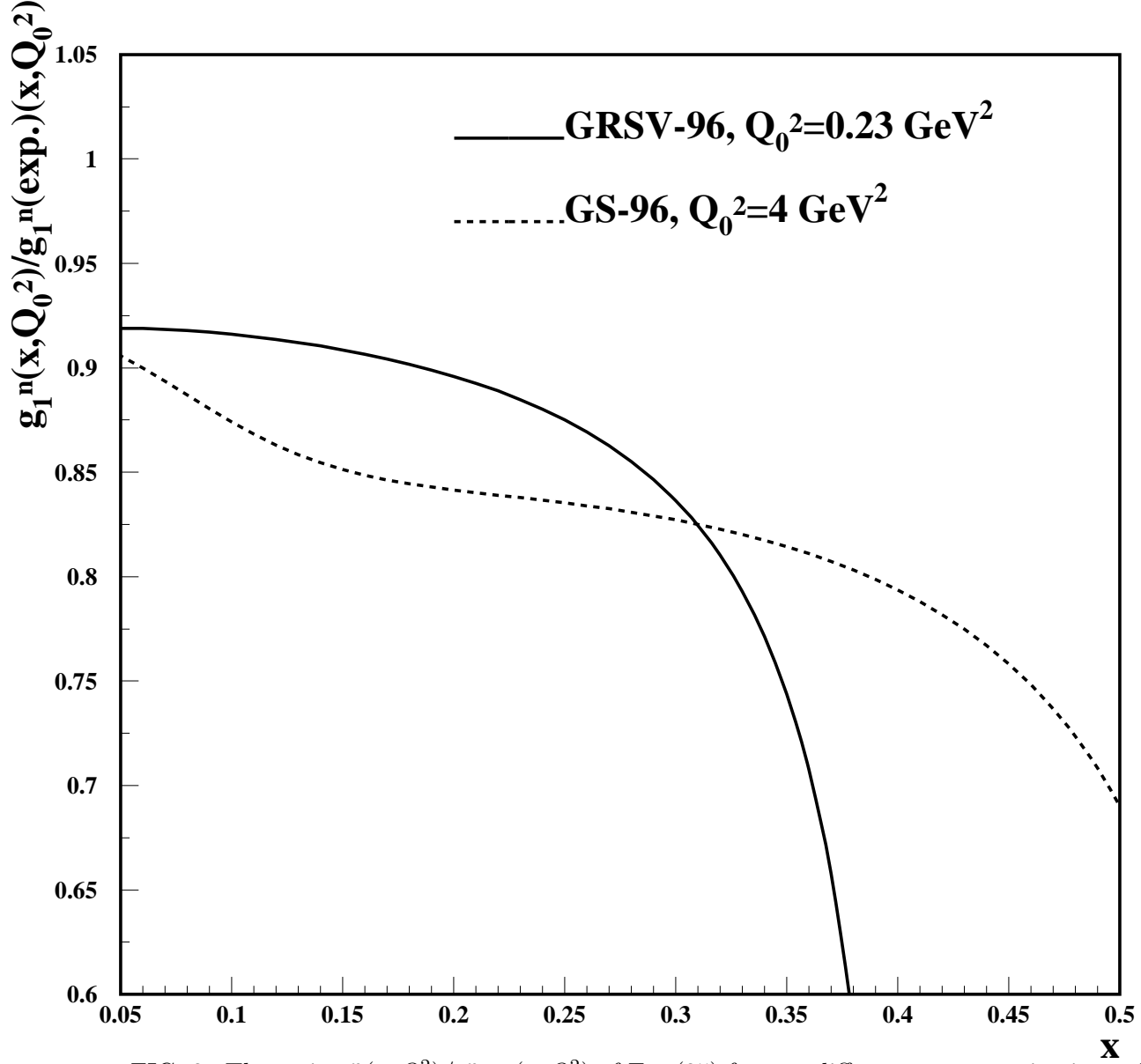


FIG. 2. The ratio  $g_1^n(x, Q^2)/g_{1exp.}^n(x, Q^2)$  of Eq. (25) for two different parameterizations of the spin-dependent parton densities at the initial scales  $Q_0^2=0.23 \text{ GeV}^2$  and  $Q_0^2=4 \text{ GeV}^2$ , respectively. This ratio would be unity if the effect of the  $\Delta$  were unimportant.

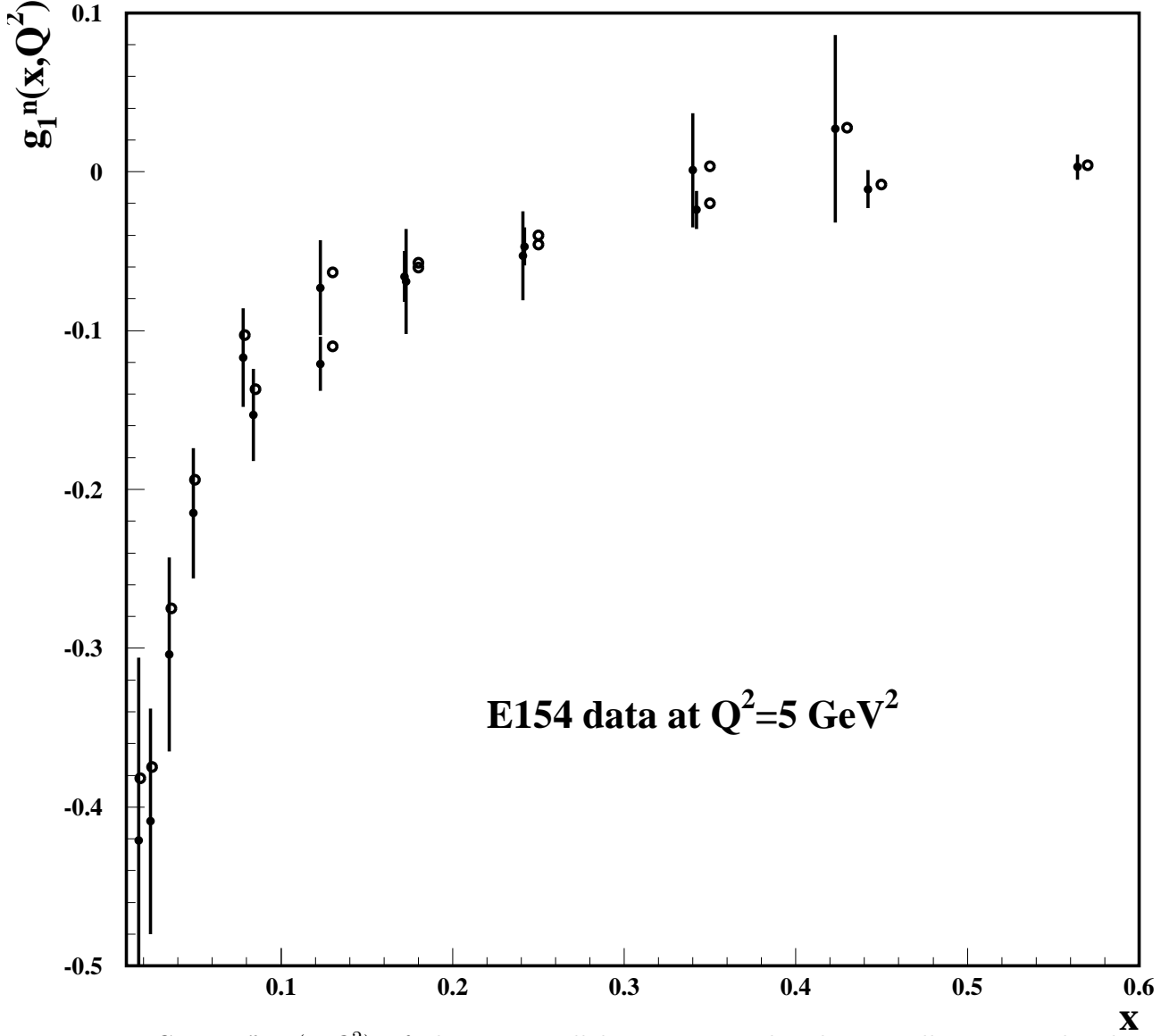


FIG. 3.  $g_{1exp}^n(x, Q^2)$  of the E154 collaboration vs. the theoretically corrected values for  $g_1^n(x, Q^2)$ , as given in Eq. (24), as functions of  $x$  at  $Q^2=5 \text{ GeV}^2$ . The experimental data points and the corresponding statistical error bars are presented as solid dots and solid vertical lines, correspondingly. The theoretically corrected values for  $g_1^n(x, Q^2)$  are given by open circles. (The open circles have been shifted to make them legible.)

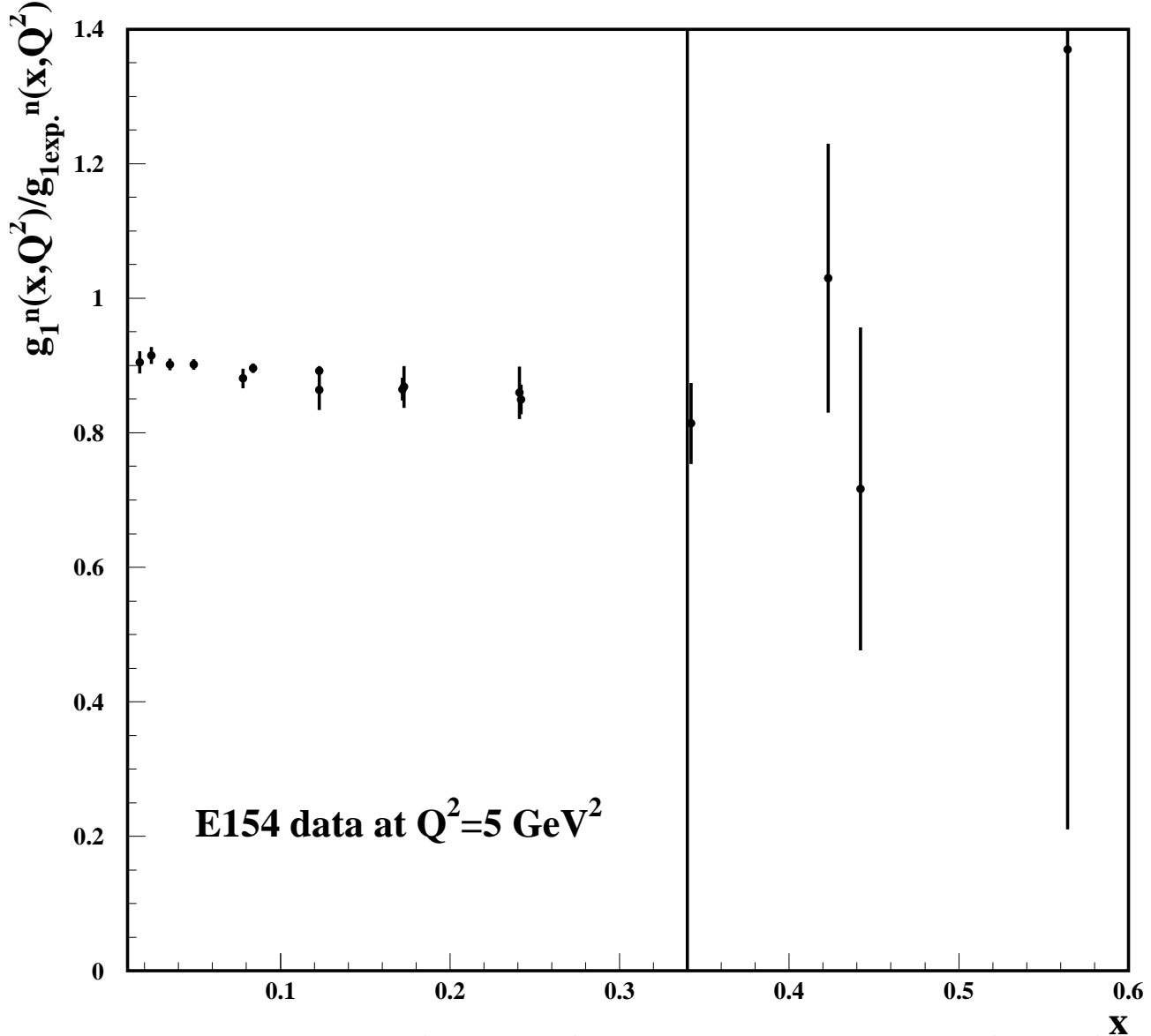


FIG. 4. The ratio  $g_1^n(x, Q^2)/g_{1exp}^n(x, Q^2)$  of Eq. (25) as a function of  $x$  at  $Q^2=5 \text{ GeV}^2$  for the E154 data. The vertical solid lines are systematic uncertainties of experimental values for  $g_1^n(x, Q^2)$  and  $g_1^p(x, Q^2)$  added in quadrature.

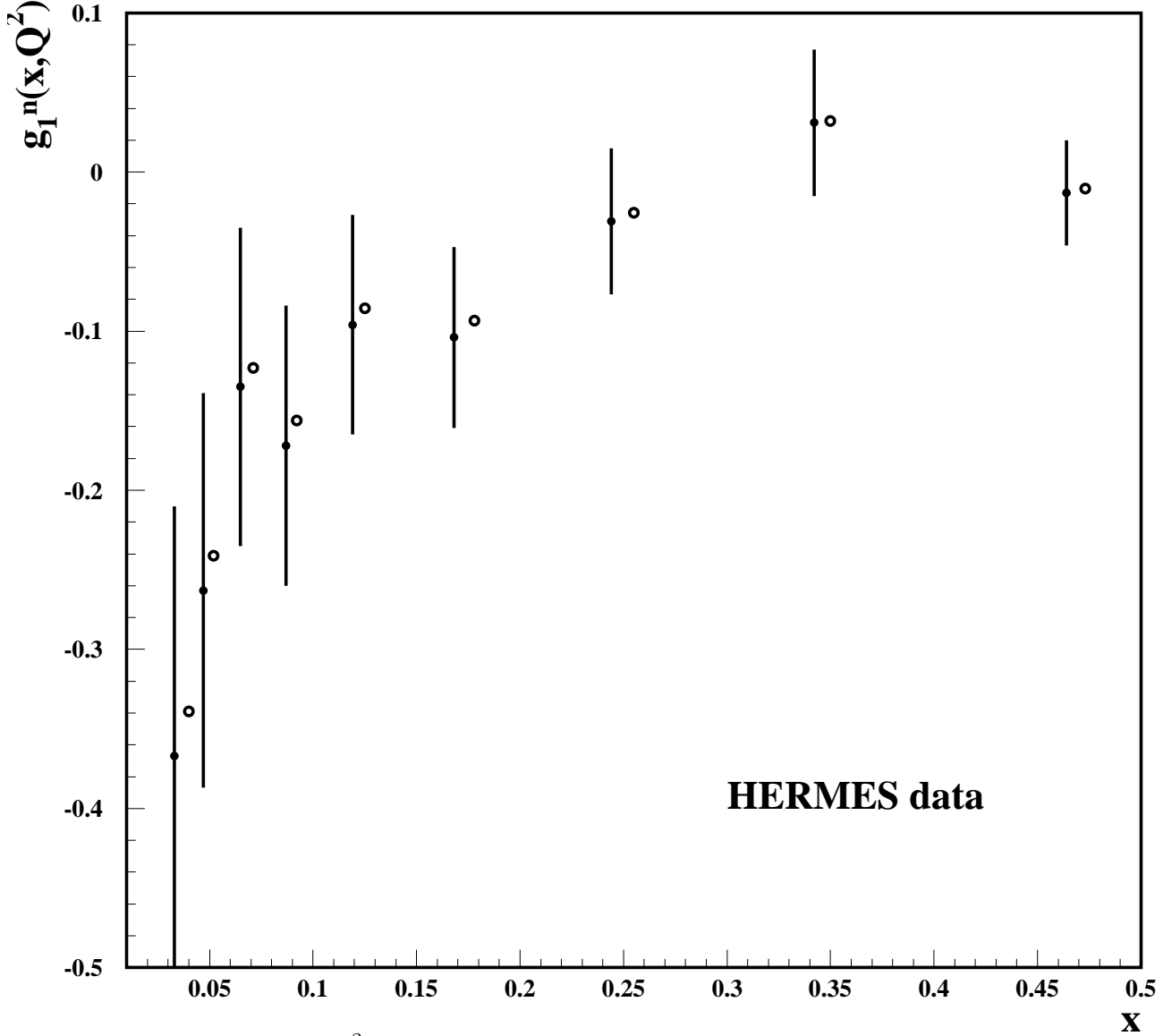


FIG. 5.  $g_{1exp}^n(x, Q^2)$  of the HERMES collaboration vs. the theoretically corrected values for  $g_1^n(x, Q^2)$ , as given in Eq. (24), as functions of  $x$  at  $Q^2$  correlated with  $x$ . The experimental data points and the corresponding statistical error bars are presented as solid dots and solid vertical lines, correspondingly. The theoretically corrected values for  $g_1^n(x, Q^2)$  are given by open circles. (The open circles have been shifted to make them legible.)

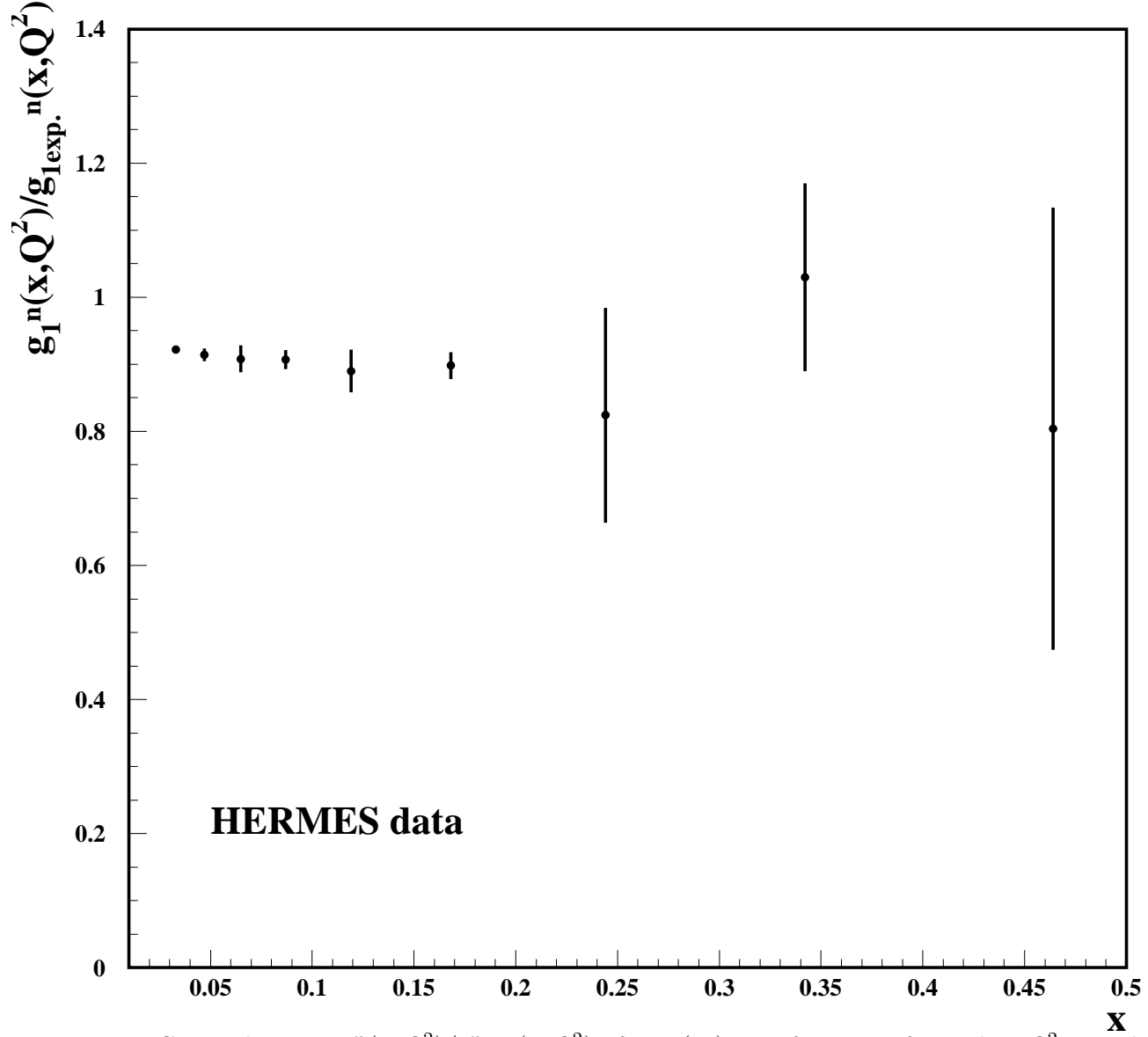


FIG. 6. The ratio  $g_1^n(x, Q^2)/g_{1exp.}^n(x, Q^2)$  of Eq. (25) as a function of  $x$  and at  $Q^2$ , correlated with  $x$  for the HERMES data. The vertical solid lines are systematic uncertainties of experimental values for  $g_1^n(x, Q^2)$  and  $g_1^p(x, Q^2)$  added in quadrature.

## REFERENCES

- [1] HERMES Collab., K. Ackerstaff *et al.*, Phys. Lett. **B 404**, 383 (1997).
- [2] E154 Collab., K. Abe *et al.*, *ibid.* **405**, 180 (1997); K. Abe *et al.*, Phys. Rev. Lett. **79**, 26 (1997).
- [3] SMC Collab., D. Adams *et al.*, Phys. Lett. **357**, 248 (1995); D. Adams *et al.*, *ibid.* **396**, 338 (1997); B. Adeva *et al.*, Phys. Rev. **D 58**, 112001 (1998).
- [4] E143 Collab., K. Abe *et al.*, Phys. Lett. **B 364**, 61 (1995); K. Abe *et al.*, Phys. Rev. Lett. **75**, 25 (1995); K. Abe *et al.*, Phys. Rev. **D 58**, 112003 (1998).
- [5] B. Blankleider and R.M. Woloshyn, Phys. Rev. **C 29**, 538 (1984).
- [6] J.L. Friar, B.F. Gibson, G.L. Payne, A.M. Bernstein, and T.E. Chupp, Phys. Rev. **C 42**, 2310 (1990).
- [7] L. Frankfurt and M. Strikman, Nucl. Phys. **A 405**, 557 (1983); W. Melnitchouk, G. Piller, and A.W. Thomas, Phys. Lett. **B 346**, 165 (1995); S.A. Kulagin *et al.*, Phys. Rev. **C 52**, 932 (1995).
- [8] C. Ciofi degli Atti, S. Scopetta, E. Pace, and G. Salme, Phys. Rev. **C 48**, R968, (1993).
- [9] T.-Y. Saito, Y. Wu, S. Ishikawa, and T. Sasakawa, Phys. Lett. **B 242**, 12 (1990); J. Carlson, D. Riska, R. Schiavilla, and R.B. Wiringa, Phys. Rev. **C 44**, 619 (1991).
- [10] L. Frankfurt, V. Guzey, and M. Strikman, Phys. Lett. **B 381**, 379 (1996).
- [11] J.D. Bjorken, Phys. Rev. **148**, 1467 (1966).
- [12] Particle Data Group, C. Caso *et al.*, Eur. Phys. J. **C 3**, 1 (1998).
- [13] B. Budick, Jiansheng Chen, and Hong Lin, Phys. Rev. Lett. **67**, 2630 (1991).
- [14] M. Gluck, E. Reya, M. Stratmann, and W. Vogelsang, Phys. Rev. **D 53**, 4775 (1996).
- [15] C. Boros and A.W. Thomas, Phys. Rev. **D 60**, 074017 (1999).

- [16] F.E. Close and A.W. Thomas, Phys. Lett. **B 212**, 227 (1988).
- [17] A.I. Signal and A.W. Thomas, Phys. Lett. **B 211**, 481 (1988) and Phys. Rev. **D 40**, 2832 (1989); A.W. Schreiber, *et al.*, Phys. Rev. **D 42**, 2226 (1990).
- [18] A.V. Manohar, 7th Lake Louise Winter Institute, eds. Campbell et al. (Lectures presented at the Lake Louise Winter Institute, February, 1992, preprint hep-ph/9204208).
- [19] V. De Alfaro, S. Fubini, G. Furlani, and C. Rossetti, 'Current in Hadron Physics', North-Holland Publishing Company, 1973.
- [20] L. Alvarez-Ruso, S.K. Singh, and M.J. Vicente Vacas, Phys. Rev. **C 57**, 2693 (1998).
- [21] T. Kitagaki *et al.*, Phys. Rev. **D 42**, 1331 (1990).
- [22] T. Gehrmann and W.J. Stirling, Phys. Rev. **D 53**, 6100 (1996).
- [23] Proposal of the E-99-117 experiment at TJNAF "Precision measurement of the neutron asymmetry  $A_1^n$  at large  $x_{Bj}$  using TJNAF at 6 GeV". Spokepersons: Z.-E. Meziani, J.-P. Chen, and P. Souder.
- [24] HERMES Collab., A. Airapetian *et al.*, Phys. Lett. **B 442**, 484 (1998).
- [25] E155 Collab., Phys. Lett. **B 463**, 339 (1999).
- [26] E143 Collab., K. Abe *et al.*, Phys. Lett. **B 452**, 194 (1999).
- [27] NMC Collab., M. Arneodo *et al.*, Phys. Lett. **B 364**, 107 (1995).